Postnatal Ontogeny of Nasal Turbinals in the Big Brown Bat, *Eptesicus fuscus*

Tim D. Smith, Kathryn E. Stanchak, Sarah E. Downing, Nicholas A. King, Veronica B. Rosenberger, Thomas P. Eiting, Abigail A. Curtis, Paul A. Faure, and Sharlene E. Santana

Volume 2, 2024 Journal of North American Bat Research No. 3

♦ The *Journal of North American Bat Research* is a peer-reviewed and edited journal for science related to all aspects of the biology, ecology, and conservation of bats, Order Chiroptera, and their habitats in North America, including Canada, Mexico, the USA, and the West Indies (Bahamas, Greater Antilles, and Lesser Antilles). (ISSN 2994-1075 [online]).

♦ The journal features research articles, notes, and research summaries on bats.

♦ It offers article-by-article online publication for prompt distribution to a global audience.

♦ It offers authors the option of publishing large files such as data tables, and audio and video clips as online supplemental files.

♦ Special issues - The *Journal of North American Bat Research* welcomes proposals for special issues that are based on conference proceedings or on a series of invitational articles. Special issue editors can rely on the publisher's years of experiences in efficiently handling most details relating to the publication of special issues.

♦ Indexing - The *Journal of North American Bat Research* is a young journal whose indexing at this time is by way of author entries in Google Scholar and Researchgate. Its indexing coverage is expected to become comparable to that of the Institute's first 3 journals (*Northeastern Naturalist*, *Southeastern Naturalist*, and *Journal of the North Atlantic*). These 3 journals are included in full-text in BioOne.org and JSTOR.org and are indexed in Web of Science (clarivate.com) and EBSCO.com.

♦ The journal's staff is pleased to discuss ideas for manuscripts and to assist during all stages of manuscript preparation. The journal has a page charge to help defray a portion of the costs of publishing manuscripts. Instructions for Authors are available online on the journal's website (https://www.eaglehill.us/nabr).

♦ It is co-published with the *Northeastern Naturalist*, *Southeastern Naturalist*, *Caribbean Naturalist*, *Eastern Paleontologist*, and other journals.

♦ It is available online in full-text version on the journal's website (https://www.eaglehill.us/nabr). Arrangements for inclusion in other databases are being pursued.

Cover Photograph: Photograph of a 6-day old *Eptesicus fuscus* pup, photographed in the laboratory of Paul A. Faure.

The ***Journal of North American Bat Research*** (ISSN 2994-1075) is published by the Eagle Hill Institute, PO Box 9, 59 Eagle Hill Road, Steuben, ME 04680-0009. Phone: 207-546-2821 Ext. 4. E-mail: office@eaglehill.us. Webpage: https://www.eaglehill.us/nabr. Published on an article by article basis. **Special issue proposals are welcome**. The ***Journal of North American Bat Research*** is an open access journal. **Authors**: Submission guidelines are available at https://www.eaglehill.us/programs/journals/nabr/nabr.shtml. **Co-published journals:** The *Northeastern Naturalist*, *Southeastern Naturalist*, *Caribbean Naturalist*, and *Eastern Paleontologist*, each with a separate Board of Editors. The Eagle Hill Institute is a tax exempt 501(c)(3) nonprofit corporation of the State of Maine (Federal ID # 010379899).

Postnatal Ontogeny of Nasal Turbinals in the Big Brown Bat, *Eptesicus fuscus*

Tim D. Smith[1,*], Kathryn E. Stanchak[2], Sarah E. Downing[3], Nicholas A. King[1], Veronica B. Rosenberger[1], Thomas P. Eiting[4,5], Abigail A. Curtis[2], Paul A. Faure[6], and Sharlene E. Santana[2,7]

Abstract - Nasal turbinals, scrolled thin bones of the nasal cavity, increase surface area for conditioning inspired air or for olfaction in mammals. To assess function in *Eptesicus fuscus* (Big Brown Bat), we quantify surface area of respiratory and olfactory turbinals from birth to adult size, using data from microCT scans before and after iodine staining. Surface area of each turbinal is significantly correlated with postnatal age and cranial length. The surface area of the maxilloturbinal and first ethmoturbinal (ET I) grows faster, relative to skull size, than surface area of caudal ethmoturbinals or the frontoturbinal. Histological examination of selected specimens reveals ET I grows disproportionately more presumptive respiratory mucosa than olfactory mucosa, supporting the hypothesis that ET I has a dual function. Lastly, we find that distribution of olfactory mucosa in the caudal nasal cavity diminishes with age. Our findings suggest a reduction in olfactory function in *E. fuscus,* perhaps due to a diminished role in food acquisition by this aerial insectivore.

Introduction

Nasal turbinals are complex projections of the lateral nasal wall that are named for the bone they articulate with (e.g., maxilloturbinals, ethmoturbinals). Although the turbinals and other internal nasal structures are bones, their function is accomplished by their mucosal covering (Bhatnagar and Kallen 1974a, Ito et al. 2021, Van Valkenburgh et al. 2011). Mucosae constitute a combination of surface epithelium and underlying soft tissues that protect core tissues from pathogens, moisten and warm inspired air, and detect external stimuli. The 2 most abundant types of mucosae are respiratory mucosa (for air conditioning) and olfactory mucosa (for odorant detection), and turbinals provide increased surface area for both functions. Across mammals, the maxilloturbinal augments respiratory air conditioning, but not olfaction (Owerkowicz et al. 2015), whereas ethmoturbinals are specialized for olfaction, although some of the latter have a dual (respiratory and olfactory) function (Smith et al. 2015, Yee et al. 2016).

Many factors influence turbinal surface area. For example, surface area of the maxilloturbinal is larger in arctic and aquatic carnivorans, compared to other members of the order, an apparent adaptation to water and/or heat loss during breathing (Green et al. 2012, Van Valkenburgh et al. 2011). Conversely, compared to terrestrial species, small mammals from aquatic and semi-aquatic habits have smaller turbinals in the olfactory region, suggesting

[1]School of Physical Therapy, Slippery Rock University, Slippery Rock, PA 16057. [2]Department of Biology, University of Washington, Seattle, WA 98195. [3]Department of Physical Therapy, Duquesne University, Pittsburgh, PA 15282. [4]Department of Physiology and Pathology, Burrell College of Osteopathic Medicine, Las Cruces, NM 88001. [5]Department of Biology, New Mexico State University, Las Cruces, NM 88001. [6]Department of Psychology, Neuroscience & Behaviour, McMaster University, Hamilton, ON L8S 4L8, Canada. [7]Burke Museum of Natural History and Culture, University of Washington, Seattle, WA 98195. *Corresponding author - timothy.smith@sru.edu.

Editor: Allen Kurta, Eastern Michigan University

reduced olfactory performance (Martinez et al. 2020). Greater surface area of olfactory turbinals has also been linked to dietary specializations, such as carnivory (Green et al. 2012, Martinez et al. 2018). Moreover, body size, especially midfacial or rostral size, is a potential constraint on the size of all turbinals (Smith et al. 2007, Van Valkenburgh et al. 2014), as shown by studies of dog breeds with different degrees of rostral projection (Wagner and Ruf 2021).

The correlation of body and midfacial size with turbinal surface area reflects, in part, a packaging dilemma: space within the nasal cavity is limited, and any constraint on midfacial volume limits available space for the turbinals that project into the cavity (Van Valkenburgh et al. 2014, Wagner and Ruf 2021). This constraining influence affects surface area of turbinals, or parts of turbinals, specialized for respiratory function differently than those specialized for olfaction, because respiratory surface area scales closer to isometry, relative to cranial measurements or body mass, than does olfactory surface area (Smith et al. 2007, Van Valkenburgh et al. 2014). The relationship of respiratory nasal surface area to body size reflects an increased demand for conditioning of inspired air; larger airway volume increases the potential for desiccation, thus requiring more respiratory mucosa, and increases demand for filtration of inhaled particles (Smith et al. 2007). In contrast, surface area of olfactory turbinals, like other sensory structures, often scales with negative allometry relative to body mass or cranial dimensions (Howland et al. 2004, Nummela 1995, Van Valkenburgh et al. 2011), presumably because sensory demands change little with increasing body size (Eiting et al. 2023, Smith and Bhatnagar 2004).

Prior studies indicate that turbinals develop (chondrify and ossify) and grow at different rates. In bats, primates, and rodents, more caudal ethmoturbinals chondrify later than more rostral ethmoturbinals (Ruf 2020, Smith and Rossie 2008, Smith et al. 2021a). In primates, the most rostral respiratory turbinal—the maxilloturbinal—undergoes prolonged postnatal bone growth, resulting in the redundant scrolling of turbinal plates called lamellae (Smith et al. 2016), and similar growth trajectories occur in *Rousettus leschenaultii* (Desmaraest) (Leschenault's Rousette) (Smith et al. 2021a). In at least some bats and primates, the unattached, freely projecting part of ET I is lined mainly with respiratory mucosa and grows more rapidly than the olfactory regions of this turbinal (Smith et al. 2007, 2021a).

Surprisingly few studies have adopted a developmental approach to understand scaling of nasal turbinals. Given differences in scaling properties and the proportion of respiratory and olfactory functions of individual turbinals, a nonuniform growth rate among nasal turbinals is expected. Any disparity in growth among turbinals may be especially pronounced postnatally, when respiratory turbinals or parts of turbinals grow rapidly and become elaborately scrolled (Smith et al. 2007, 2021a). Because this growth pattern also is true in birds (Hogan et al. 2020), scrolling likely relates to an air-conditioning role (warming and humidification) for respiratory turbinals in endothermic vertebrates.

Here, we quantify the surface area of turbinals across postnatal age in a vespertilionid bat, *Eptesicus fuscus* (Palisot de Beauvois) (Big Brown Bat). Bats are interesting organisms for the study of nasal scaling because they are small sized, with a median body mass of only 16.2 g (Jones and Purvis 1997), potentially accentuating the packaging dilemma. Indeed, because of small body and head size, the competing demands of multiple skull functions (e.g., hearing, olfaction, echolocation, and mastication) may increase the likelihood that specialization in 1 structure requires a trade-off, modifying or even reducing other structures (Hedrick and Dumont 2018; Pedersen 1993, 1995; Santana and Miller 2016). Although some bats have the presumed plesiomorphic number of turbinals for mammals, many have fewer (Allen 1882, Bhatnagar and Kallen 1974b), perhaps because they exhibit

reduced midfacial projection (Camacho et al. 2020, Dzal and Gillam 2023). *E. fuscus* is additionally of interest because it is insectivorous, and insectivory correlates with reduced olfactory structures (Bhatnagar and Kallen 1974a, b; Eiting et al. 2023). Using microCT (microcomputed tomography) and diceCT (diffusible iodine-based contrast-enhanced computed tomography), as well as histology of selected matching specimens, we test whether the turbinals of this bat are characterized by lower growth rates of olfactory structures relative to respiratory structures (as described above in primates). Additionally, we predict that the first ethmoturbinal grows mostly in its respiratory regions, as in other mammals.

Methods

Terminology of the nasal cavity

The nasal cavity is divided into right and left nasal fossae, each of which shares the nasal septum as its medial border. In most mammals, 4 ethmoturbinals project from the lateral wall of the nasal cavity toward the septum, along with 1 or more frontoturbinals, 1 maxilloturbinal, and a variable number of smaller interturbinals (Smith et al. 2015). At the caudal end of the nasal cavity, on each side, the airway divides into 2 regions: a dorsal cul-de-sac, called the olfactory recess, and a ventral nasopharyngeal duct, which is continuous with the pharynx caudally (Smith et al. 2015).

Among bats, pteropodid species possess a full complement of all types of turbinals; however, most other species, including *E. fuscus*, have lost at least 1 ethmoturbinal. Ethmoturbinals are traditionally identified using Roman numerals; in our study, we ignore the question of which ethmoturbinal (ET) is missing in *E. fuscus,* and name the 3 that are present, from front to back, as ET I, ET II, and ET III.

Composition of the sample

We used microCT and diceCT scans of an ontogenetic series of subadult *E. fuscus* that were previously prepared for a study of masticatory muscles (Santana 2018, Stanchak et al. 2023). From that sample, we selected 7 specimens, based on discernability of nasal tissues versus surrounding airways in diceCT scan slices. These 7 animals were taken from a captive colony at McMaster University at 0 (neonate), 7, 14, 20, 28, 35, and 42 days after birth; the 28- and 42-day-old specimens were female, and the rest were male (Stanchak et al. 2023). Members of this colony weighed about 3.6 g at birth and reached approximately 17–19 g after 45 days, with females larger than males (Mayberry and Faure 2014). We also qualitatively examined histological sections from 4 adult *E. fuscus* (1 male and 3 unrecorded sex) that had been prepared for earlier an study (Bhatnagar 1980).

Computerized visualization and histology

Heads were fixed in 4% paraformaldehyde in phosphate-buffered saline and imaged in a microCT scanner (SkyScan 1172, Bruker Corporation, Billerica, MA), with scan parameters that ranged from 29 to 55 kV and 175 to 181 μA. To aid in visualizing soft-tissue structures, heads were then immersed in a solution of either 1% weight/volume (0- and 7-day-old specimens) or 3% weight/volume (all others) of Lugol's iodine for 5–11 days and rescanned (Gignac et al. 2016, Stanchak et al. 2023). Some shrinkage is associated with iodine staining (Hedrick et al. 2018). However, prior work showed that iodine-related shrinkage is less than with other methods, such as histology, with respect to measurements of nasal mucosa (Smith et al. 2021b).

After scanning, we assembled raw scan data into stacks of bitmap images, using the software NRecon (Bruker Corporation). Data and images from the microCT scans have

been placed online (https://www.morphosource.org, under the project title "*Eptesicus fuscus* ontogenetic series of heads"). We used Amira software (Thermofisher, Pittsburgh, PA) to reconstruct the 3-dimensional structure of the skull and nasal fossa from microCT and diceCT scans, respectively. We assessed age-related changes in turbinal size and epithelial surface area relative to 2 cranial dimensions. To estimate skull and rostral size, we generated a 3-dimensional reconstruction of each skull from micro-CT scans, using the Label Voxels tool to set a threshold for greyscale values representing bone versus air. Then we used the Volume tool to generate a 3-dimensional model of the skull.

We determined palatal and cranial lengths with the 3D Measure tool in Amira. Because a midline gap occurs in the upper jaw of vespertilionid bats, a virtual bar was created between the anterior ends of the right and left premaxilla, and the rostralmost point for each length was placed at the center of the bar. We defined cranial length as the distance between this bar and the inion at the convergence of the nuchal lines of the occipital bone. Palatal length, which was a proxy for rostral length, was measured between the virtual point and the posterior midpoint of the hard palate.

To reconstruct the soft-tissue boundaries of the walls of the nasal fossa from diceCT scans, we first selected airways according to their highly radiolucent (darker gray) appearance compared to iodine-stained soft tissues, using Amira's Magic Wand tool, or manually tracing when necessary (e.g., when mucus or other artifactual substances were stained with iodine). Similarly, we outlined all soft tissues based on their lighter gray appearance. Volumes of both airway and soft tissue were saved as separate files, and hereafter, we use the term "volume" in lieu of the Amira file type that stored the space occupied by structures observed in CT slices. The airway volume was then subtracted from the soft-tissue volume to remove noise near the mucosal surface. Sources of noise included scattered radiation during scanning and secreted material, such as mucus, both of which created artificial irregularities in the surface contours of turbinals.

We exported individual CT slices, which included only the regions designated as soft tissue, as binary TIFF files. To quantify mucosal surface area for each turbinal, we imported the files into ImageJ (https://imagej.net), measured turbinal perimeters slice by slice (Fig. 1), and then multiplied perimeters by interslice distance to calculate surface area. All CT scans were reconstructed in the coronal plane, approximately perpendicular to the palatal plane.

To visualize age-related change in olfactory mucosa on the ethmoturbinals, we decalcified the heads of the 3 youngest specimens (0-, 7- and 14-days old). Each was embedded in paraffin, serially sectioned at 10-µm thickness, and stained using Gomori trichrome and hematoxylin-eosin; the 4 adults had already been processed in a similar manner (Bhatnagar, 1980). Histological sections of the subadults were examined to detect mucosal changes in diceCT slices in the same (frontal) plane. When the plane of the CT slice was not oriented similar to the histological sections, we rotated the diceCT scan volume using Amira, until the slice plane matched the histological section (see Supplemental File 1, available online at http://www.eaglehill.us/NABRonline/suppl-files/nabr-008-Smith-s1), and the volume was resliced in the matching plane.

In the 3 youngest specimens, diceCT slices were annotated to allow us to measure the extent of olfactory and respiratory mucosa lining the ethmoturbinals. Unless we specifically discuss histological sections, we use the term "nonolfactory" instead of respiratory, because only olfactory mucosa was identified using diceCT. Initially, we compared diceCT slices to histological sections at similar cross-sectional levels and noted that olfactory mucosa was distinctly thicker than nonolfactory mucosa, and similarly, Smith et al. (2021b) showed that the olfactory epithelium and supporting glands were thick and radiopaque in diceCT scan

slices. Consequently, in our study, we identified olfactory mucosa in diceCT scans based on its greater thickness (see Supplemental File 1, available online at http://www.eaglehill.us/NABRonline/suppl-files/nabr-008-Smith-s1).

We manually annotated olfactory mucosa using a paint brush tool in Amira; marking was done every 2–3 slices and interpolated. Next, the previously captured nasal airway volume was subtracted from the olfactory mucosa volume to ensure the annotations were flush with the surface of the soft-tissue volume. We then exported the olfactory mucosa volume as TIFF files representing individual CT slices containing olfactory mucosa. Using Photoshop (Adobe, San Jose, CA), we superimposed the olfactory-mucosa TIFFs over soft-tissue images, and the color of the olfactory mucosa was changed to create an annotating boundary denoting the perimeter of the olfactory surface in each slice. We identified the precise rostral and caudal end points of olfactory mucosa and otherwise manually measured the perimeter every 3–4 slices in ImageJ. Due to damage of the rostralmost sections of ET II in the 14-day-old, we only reconstructed and measured areas of ET I and ET III.

The 4 adults had not been diceCT scanned, so they could not be used for 3-dimensional reconstructions. However, we combined histological information from those previously prepared adults with data from the youngest subadults, to assess age-related changes in rostrocaudal distribution of olfactory and respiratory mucosa on ethmoturbinals and in the olfactory recess. In histological sections, respiratory mucosa is recognized by having an epithelium with rows of short cilia for propelling mucus that traps inhaled particles, and a

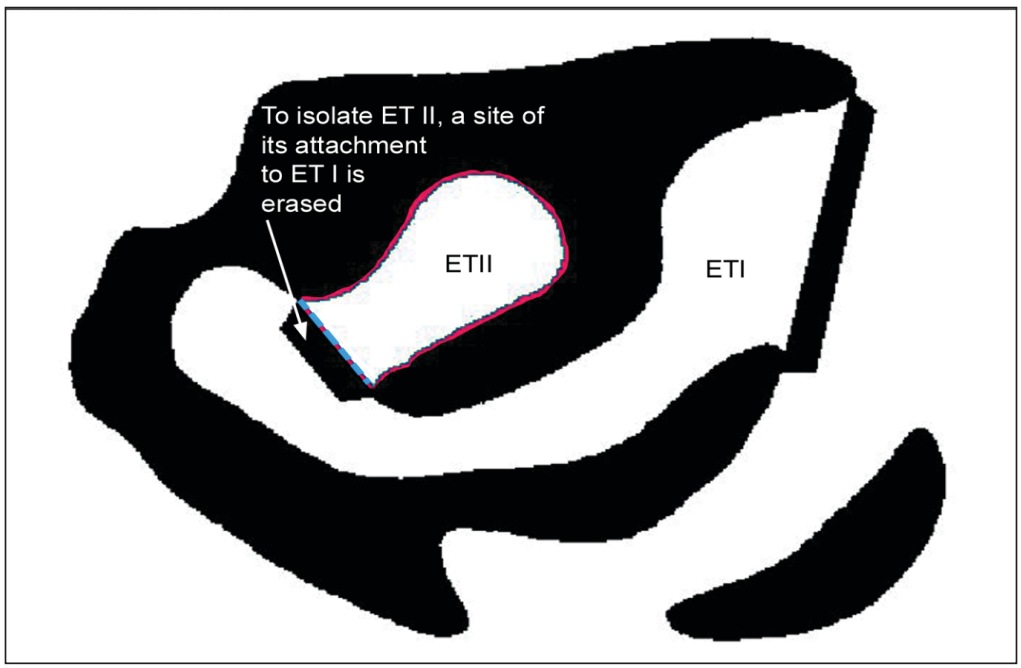

Figure 1. To measure turbinal surface area, we first converted CT slices to binary files and measured turbinal perimeter. In this example, the second ethmoturbinal (ET II) is isolated from its attachment to the first ethmoturbinal (ET I), and total perimeter of ET II (red outline) was measured using ImageJ. Then, the length of the base (dashed blue line) was measured and subtracted to obtain the actual perimeter of ET II, excluding its attachment site. Perimeter was multiplied by interslice distance and summed to obtain surface area. Black represents nasal airway, whereas white within the airway represents turbinals covered with mucosa.

highly vascular mucosa for warming inspired air. Olfactory mucosa, in contrast, has a thick epithelium because it has multiple rows of cell bodies of the sensory neurons; the connective tissue deep to this epithelium is also thick, because it contains Bowman's glands and olfactory nerves (Harkema et al. 2006).

Statistics

A Shapiro-Wilk test indicated that no variables differed significantly from a normal distribution. We examined the relationship of square root of turbinal surface area versus cranial length using ordinary least-squares linear regression, to obtain slopes for comparisons among variables. We used Pearson's correlation coefficient (r), to evaluate the strength of the relationship. Because snout dimensions influence turbinal size and morphology (Yee et al. 2016), we also assessed changes in palatal length with age. We used Excel (Microsoft, Redmond, WA, USA) to obtain correlation coefficients and R (vers 4.3.1; R Core Team 2024) to calculate regressions. Because we used square root of area, a slope of 1 was expected for an isometric relationship with cranial or palatal length; we predicted that the turbinals with more nonolfactory mucosa and were most rostrally positioned (ET I and maxilloturbinal) would scale closer to isometry than those that were mostly covered with olfactory mucosa and positioned dorsocaudally (ET II, ET III, and the frontoturbinal). Alpha was set at 0.05 for all procedures.

Results

Quantitative changes in turbinal surface area across age

All turbinal surface areas are significantly correlated (Table 1) with postnatal age (r = 0.87–0.98) and cranial length (r = 0.93–0.96), as is palatal length with cranial length (r = 0.99). Slopes of regression lines for area of the rostral maxilloturbinal and ET I against cranial length (0.37 and 0.44, respectively) are more than double the slopes for any other turbinals (Table 1; Fig. 2), although we are unable to test for statistical differences due to small sample sizes. The slope for palatal length against cranial length is 0.67 (Table 1).

Morphogenesis of ethmoturbinals and the olfactory recess

Qualitative comparisons indicate that the rostral end of ET I grows rapidly between birth and 14 days (Fig. 3), expanding the amount of the rostral tip that is solely lined with nonolfactory mucosa (Figs. 3 and 4a–c). The shape of ET I also changes with age, becoming more elongated rostrocaudally and folded ventrally (Fig. 3b). In contrast, ET II and ET III retain nearly the same proportions across ages (Figs. 3a–b), consistent with apparent differences in slopes among the 3 ethmoturbinals (Fig. 2). Initially, the medial and lateral edges of ET I are horizontally oriented (Figs. 3c and 4a), but ventral folding begins within the first week (Fig. 3d). These edges grow downward as descending lamellae during the first 2 weeks and become intimately folded around the maxilloturbinal (Figs. 3d and 4a–b). In histological sections from adults, this close association is enhanced by further extension of the lamellae, along with outgrowth of the maxilloturbinal (Fig. 4c). Histological examination reveals that the maxilloturbinal and the descending lamellae of ET I bear a highly vascular respiratory mucosa in the adult (Fig. 5a).

Rostrocaudal changes in distribution of olfactory and nonolfactory mucosa

In linear distribution, nonolfactory mucosa increases on the rostral end of ETI with age. At birth, 4% of the rostral end is lined with only nonolfactory mucosa; this coverage increases to

6% at 7 days and 20% at 14 days. Our measurement of a histologically sectioned adult also reveals that 20 % of the rostral end of ET I is lined with only nonolfactory mucosa (Fig. 5b). In subadults and adults, all other ethmoturbinals and the frontoturbinal have an olfactory mucosa extending closer to, if not reaching, their rostral end (Figs. 3 and 5b).

The age-related increase in linear extent of nonolfactory epithelium on the rostral end of ET I suggests that the percentage of olfactory mucosa decreases. Although total surface area of olfactory mucosa on ET I increases with age (Table 1), the percentage of olfactory mucosa on ET I decreases over 3 percentage points (41.7% to 38.0%) during the first 2 postnatal weeks (Table 2). Furthermore, if we measure only the free projection of ET I (i.e., excluding the caudal part that anchors it to the nasal cavity wall), a more precipitous decrease in olfactory surface area emerges; the 14-day-old has about 8% less surface covered by olfactory mucosa compared to the newborn (Table 2). In contrast, the percentage of ET III lined with olfactory mucosa remained nearly the same in both the neonatal and 14-day-old pups.

The olfactory recess of *E. fuscus* contains only the most caudal part of the last ethmoturbinal (III) in specimens at all ages (Figs. 4d–f). In our histologically sectioned specimens, the olfactory mucosa retreats from this caudal end of ET III and is replaced by nonolfactory tissue in the older specimens (Figs. 6a–d). In adults examined histologically, the caudal portion of ET III that lacks olfactory mucosa may amount to more than 20% of total turbinal length (Fig. 5b). Moreover, olfactory mucosa is present at birth and 7 days in the very caudal end of the recess that is devoid of turbinals; the epithelium in this region is thick, due to rows of receptor cells, and there is a thick layer of soft tissue deep to the epithelium containing glands and olfactory nerves (Fig. 6e). However, in the 14-day-old (Fig. 6f) and adults (Fig. 6g), only a thin nonolfactory epithelium is present, and little soft tissue resides between this epithelium and bone.

Table 1. Regression equations for plots of square root of turbinal surface area against age and cranial length.

Independent variable	Dependent variable	Intercept	Slope	*P*	*r*
Age	Ethmoturbinal I	3.24	0.06	< 0.001	0.96
Age	Ethmoturbinal II	1.42	0.03	< 0.002	0.94
Age	Ethmoturbinal III	1.09	0.02	< 0.005	0.91
Age	Maxilloturbinal	1.89	0.05	< 0.001	0.96
Age	Frontoturbinal	1.57	0.02	< 0.003	0.93
Age	Palatal length	6.68	0.09	< 0.001	0.96
Cranial length	Ethmoturbinal I	-3.17	0.44	< 0.001	0.96
Cranial length	Ethmoturbinal II	-1.46	0.19	< 0.001	0.96
Cranial length	Ethmoturbinal III	-1.16	0.15	< 0.002	0.94
Cranial length	Maxilloturbinal	-3.48	0.37	< 0.001	0.98
Cranial length	Frontoturbinal	-0.72	0.16	< 0.01	0.88
Cranial length	Palatal length	-2.92	0.66	<0.001	0.99

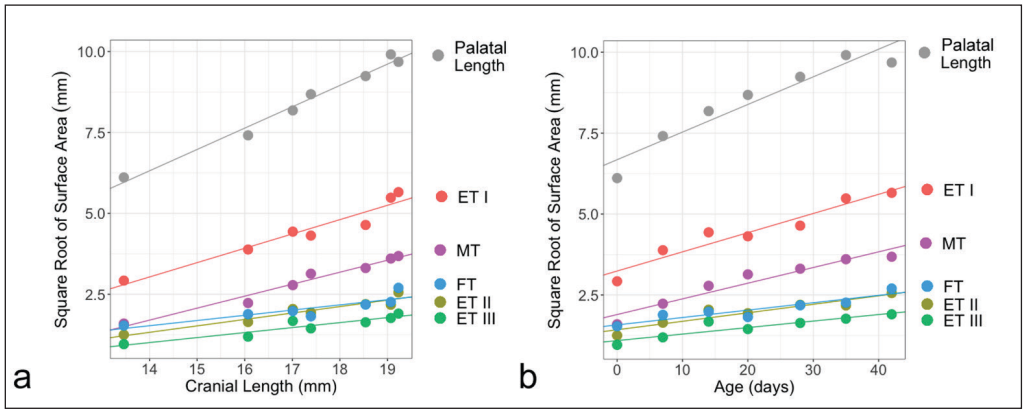

Figure 2. Palatal length and square root of turbinal surface area plotted against cranial length (a) and age (b). ET, ethmoturbinal; FT, frontoturbinal; MT, maxilloturbinal.

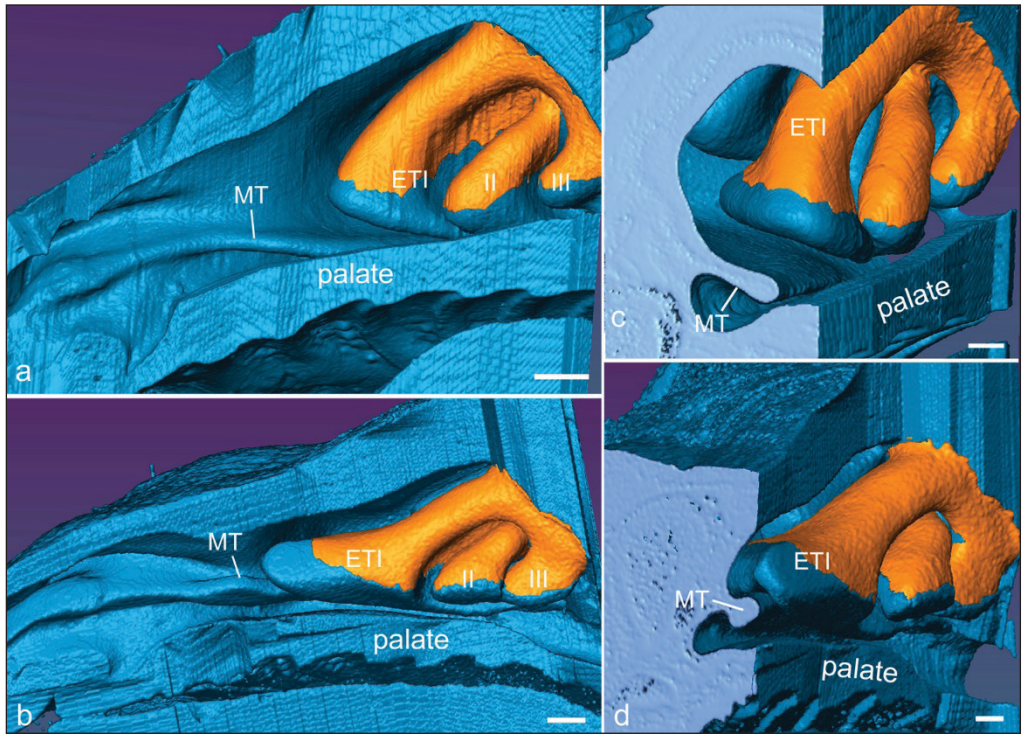

Figure 3. Three-dimensional reconstructions, generated from diceCT scans, of the lateral nasal wall and surrounding tissues in neonatal (a, c) and 14-day-old *E. fuscus* (b), highlighting distribution of the olfactory mucosa (orange) on the ethmoturbinals (ET). In the lateral views (a, b), proportional changes during the first 2 weeks are evident, including more rapid growth of ET I compared to ET II and ET III. In addition, ET I grows disproportionally into the nonolfactory mucosa on the rostral end (b). The rostromedial perspectives (c, d) reveal that ET I and the maxilloturbinal (MT) are adjacent at birth (c), but over the first 2 weeks, ET I wraps ventrally, curving around the MT (d). Scale bars: a and b = 0.5 mm; c and d = 0.25 mm.

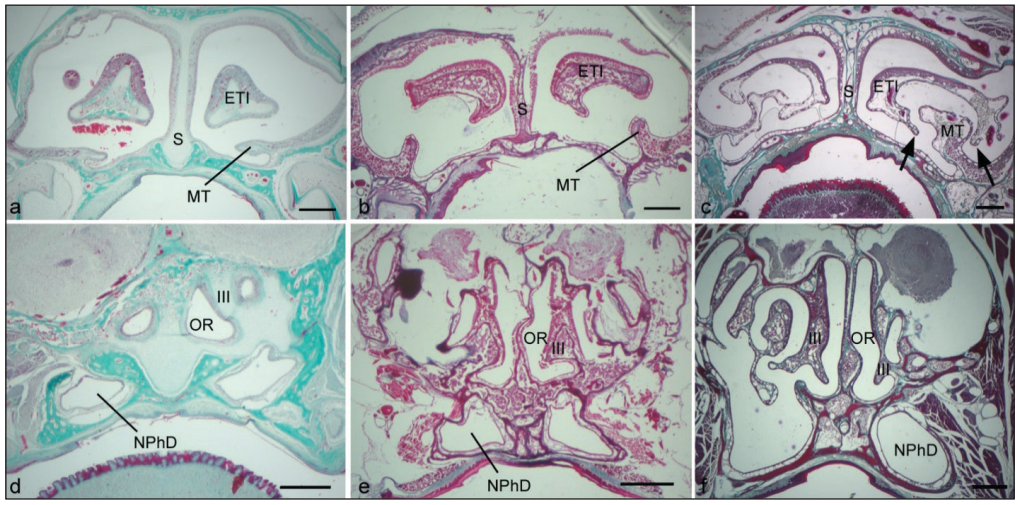

Figure 4. Histological sections of the first (ET I) and last (ET III) ethmoturbinal at birth (a, d), in a 14-day-old (b, e) and adult (c, f) *E. fuscus*. a) At birth, ET I is nearly flat along its ventral surface. b) By 14 days, ET I is concave where it faces the maxilloturbinal (MT); shrinkage caused by ethanol baths during histology make ET I and MT appear farther apart than in Figure 3c). In the adult, the lateral and medial lamellae (arrows) have grown farther ventrally, and the MT has grown medially to increase the spatial adjacency of the 2 structures. Figures 4d–f show the olfactory recess (OR) at each age. Regardless of age, only the caudalmost end of ET III is within this recess. NPhD, nasopharyngeal duct; S, nasal septum. Scale bars = 0.5 mm.

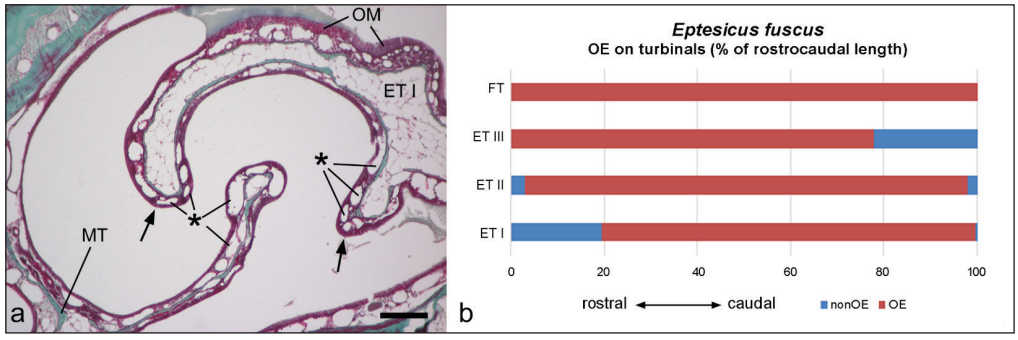

Figure 5. Mucosal covering of various turbinals in adult *E. fuscus*. a) The section is at about the 20th percentile of rostrocaudal length of ET I, where a small patch of olfactory mucosa (OM) first appears; the medial and lateral lamellae (arrows) project ventrally and are lined with respiratory mucosa. Note that the ethmoturbinal wraps around the maxilloturbinal (MT). The mucosa of MT and most of ET I possesses numerous venous sinuses (*). Scale bar = 150 µm. b) This chart shows the type and amount of epithelium, determined by histology, that is present on 4 turbinals. Approximately 20% of the rostralmost part of ET I is lined with nonolfactory epithelium (nonOE), whereas ET II and ET III have more nonolfactory epithelium on their caudal ends, compared to ET I. The frontoturbinal (FT) has olfactory epithelium (OE) along its entire extent.

Discussion

Prior studies on mammals established a stronger link between body or midfacial size and "respiratory turbinals" than "olfactory turbinals" (Green et al. 2012, Owerkowicz et al. 2015). However, it may be unreliable to employ some of the turbinals as osteological proxies for 1 particular function (respiratory or olfactory). Histological data on mammals have long confirmed that some turbinals of the ethmoid have both respiratory and olfactory functions (Bhatnagar and Kallen 1975, Loo 1974, Smith et al. 2007, Yee et al. 2016). Although *E. fuscus* resembles most mammals in this respect, we found other features that diverge from most other mammals.

Growth of turbinals in the context of function

The data presented here are the first to quantify the development of nonolfactory and olfactory surface areas and the skeletal structure of the turbinals in an ontogenetic sample from an insectivorous bat. The predictions that we made based on other vertebrates are

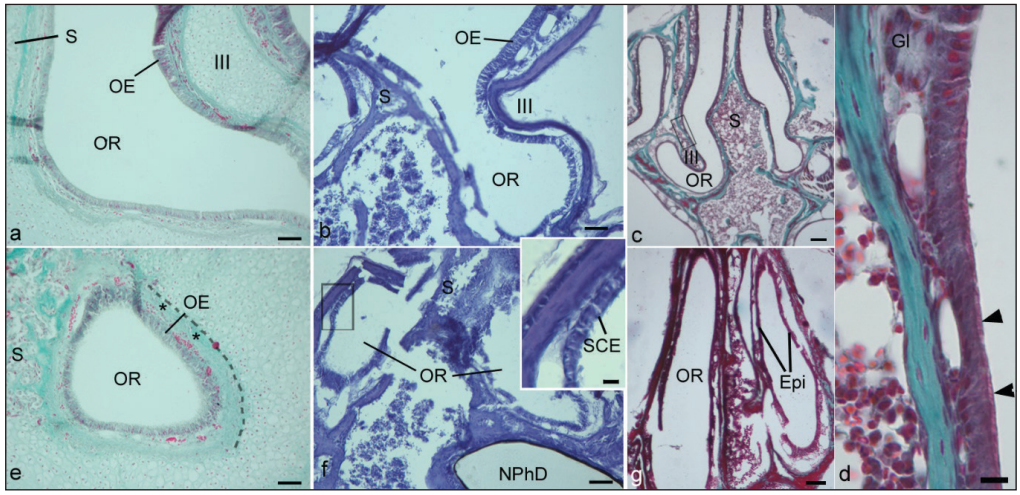

Figure 6. Histological sections of the olfactory recess (OR) in a neonate (a, e), 14-day-old (b, f) and adult (c, d, g). Photos in the top row (a–c) show a cross section through the caudal end of the last ethmoturbinal (ET III), whereas those in the bottom row (e–g) are caudal to ET III. A thick olfactory mucosa covers most of ET III in the neonate (a), is present only on the dorsal part of ET III in the 14-day-old (b), and is lacking in adults (c). The boxed region in (c) is enlarged in (d), and shows Bowman's glands (Gl) at the lower margin of the olfactory mucosa, just dorsal to ET III, which is lined by a thinner mucosa with rows of cilia (arrowheads) along the apex of the epithelium. Caudal to ET III, the OR ends as a simple cul-de-sac; the OR is lined with a thick olfactory epithelium (OE) laterally in the neonate (e), but olfactory mucosa is lacking in the 14-day-old (f). The neonate (e) also has a dense layer of soft tissue (*), containing olfactory nerves and glands, between the OE and the surrounding cartilage (cartilaginous border indicated by dashed line). The inset in (f) is a magnified view of the boxed region in that photo and shows only nonolfactory epithelium, specifically a simple cuboidal epithelium (SCE), in the 14-day-old. In the adult (g), the caudal end of the OR is lined with a uniformly thin, nonolfactory epithelium (Epi), with barely any soft tissue between it and the surrounding bone. NPhD, nasopharyngeal duct; S, nasal septum. Scale bars: a, b, e, and f = 50 µm; c and g = 150 µm; insets = 10 µm.

Table 2. Total surface area (mm^2), olfactory surface area, and percent covered by olfactory mucosa for ethmoturbinals I and III, in the youngest specimens studied.

A. Surface area (mm^2) of ethmoturbinals I and III

	Ethmoturbinal I			Ethmoturbinal III		
Age (days)	Surface area	Olfactory surface area	Percent olfactory surface	Surface area	Olfactory surface area	Percent olfactory surface
0	8.54	3.56	41.7	0.92	0.37	40.2
7	15.07	5.99	39.7	1.42	0.711	50.1
14	19.67	7.47	38	2.81	1.09	38.8

B. Surface area (mm^2) of free projections [1] of ethmoturbinals I and III

	Ethmoturbinal I			Ethmoturbinal III		
Age (days)	Surface area	Olfactory surface area	Percent olfactory surface	Surface area	Olfactory surface area	Percent olfactory surface
0	4.66	2.12	45.5	0.37	0.14	37.8
7	8.94	3.8	42.5	0.19	0.047	24.7
14	17.37	6.47	37.2	1.13	0.36	31.9

[1]The part that projects rostral to the attachment to the lateral wall.

largely supported. However, no turbinals scale with isometry relative to cranial length. Indeed, even palatal length scales with negative allometry (slope = 0.67; Table 1), suggesting that growth of the rostrum does not keep pace with the overall cranium, perhaps supporting the idea that the nasal region of this bat grows under a "packaging" constraint. However, we show differential growth of the mucosae across age. The 2 turbinals that bear the most nonolfactory mucosa, the maxilloturbinal and ET I, grow faster in surface area (relative to cranial length) than the more caudal turbinals of the ethmoid. Although ET II and III bear proportionally more olfactory mucosa than ET I, an intriguing finding is that much available space in the caudal nasal fossa is not lined with olfactory mucosa in adults, in stark contrast to most mammals (Smith et al. 2015).

We also reveal that ET I grows faster than the more caudal turbinals (Fig. 2; Table 1), and histological data from a small subset of our sample suggest that regions with different types of mucosa grow at different rates. Beyond an increase in surface area, ET I and the maxilloturbinal transform profoundly within the first week of postnatal life. Initially ET I and the maxilloturbinal are spatially separated (Figs. 3c and 4a). By 7 days, though, the lateral and medial margins of the rostral end of ET I wrap around the maxilloturbinal. This is consistent with the suggestion of Coppola et al., (2014) that the initiation of respiration is an important factor in turbinal morphogenesis and that respiratory airflow may be a mechanical stimulus that promotes turbinal growth. The functional significance of the resulting anatomical proximity is that inspired air passes through the cleft between the 2 bones and is warmed by the highly vascular mucosa that lines each turbinal (Fig. 5a).

Rostrocaudal distribution of olfactory mucosa shifts with age

Weiler and Farbman (1997) demonstrated that, as laboratory-bred *Rattus norvegicus* (Berkenhout) (Norway Rat) ages, the largest cross-sectional perimeter of olfactory mucosa shifts posteriorly, implying that, as the snout grows, the tissue responsible for the detection of odorants progressively shifts to the rear. In adult strepsirrhine primates, such as *Microcebus murinus* (Miller) (Gray Mouse Lemur), olfactory mucosa is also disproportionately caudally distributed (Smith et al. 2014).

The dorsal and caudal location of olfactory mucosa in the nasal cavity, and specifically within the olfactory recess, reflects a plesiomorphic arrangement of the nasal cavity of crown mammals; this anatomical organization maximizes access of olfactory receptor cells to inhaled odorants (Eiting et al. 2014a, Smith et al. 2019). One or more of the most caudal turbinals (in typical mammals, ET IV and possibly others) are sequestered within the olfactory recess. Not surprisingly, the most caudal ethmoturbinal has olfactory mucosa covering its entire dorsal surface, from the rostral to caudal ends, in most mammals (Adams 1972, Martinez et al. 2020, Smith and Rossie 2008, Yee et al. 2016). The sequestering of 1 or more turbinals into the olfactory recess characterizes rodents, carnivorans, ungulates, strepsirrhine primates, and other mammals, revealing an important adaptation for predator and prey species (e.g., Adams 1972, Smith and Rossie 2008, Smith et al. 2019, Yee et al. 2016).

As an adult, *E. fuscus* deviates from the primitive mammalian arrangement in 2 ways. First, the olfactory recess is exceedingly small, housing only the most caudal extent of ET III. Second, our cross-sectional age sample reveals that the most caudal ethmoturbinal (ET III) develops atypically for mammals. Although our 3 youngest specimens have the caudal ends of ET III lined with olfactory mucosa, none of our adults did. Since the caudal end of the olfactory recess bears olfactory mucosa in both newborn and 7-day-old pups, but not in the 14-day-old, posterior growth of olfactory mucosa apparently does not keep pace with

posterior expansion of the nasal cavity as a whole. Therefore, the olfactory recess has lost its ancestral function of odorant detection in adult *E. fuscus*.

Growth of the olfactory surface area in bat pups, on turbinals and elsewhere in the nasal cavity, is likely influenced by selection on social behavior as well as diet. Pups of *E. fuscus*, tested for their ability to discriminate between maternal odors and those of other females, show no preference from birth until 20 days (Mayberry et al. 2014), although olfaction in adults is related to social interactions (Bloss et al. 2002, Kilgour et al. 2013). Nevertheless, insectivorous bats have smaller olfactory bulbs compared to frugivorous bats (Bhatnagar and Kallen 1974b, Eiting et al. 2023), and we suggest that the olfactory recess of *E. fuscus* has lost its plesiomorphic olfactory function, due to the use of echolocation and the diminished importance of olfaction in hunting flying insects. However, further investigations are needed of other vespertilionids, as well as members of other families, which vary in the extent of olfactory mucosa lining the olfactory recess (Eiting et al. 2014b).

Conclusions and future directions

Our results support the hypothesis that respiratory and olfactory surfaces of nasal turbinals grow at different rates. Furthermore, our results are consistent with prior findings on primates indicating that ET I grows more rapidly than more caudal ethmoturbinals and that such growth is disproportionately occurring in respiratory regions of this turbinal. However, our results also suggest some reduction of olfactory function, perhaps due to the diminished role of olfaction in food acquisition by this aerial insectivore.

Ontogenetic studies of nasal development in bats are rare (e.g., Smith et al. 2021a). Future work should consider turbinal development, as well as changes in degree of complexity in the adult nasal cavity, especially within the context of varying facial projection among chiropterans. With our limited sample, we cannot provide robust estimates of populations of olfactory sensory neurons across age, but a future examination of these cells, as well as physiological data from *E. fuscus*, could further contextualize our findings and provide insightful comparisons to the large existing literature on rodents (Alberts 2007, Apfelbach et al. 1991, Weiler and Farbman 1997).

Acknowledgments

This study was funded by National Science Foundation grants IOS-2202272 and BCS-1830919, awarded to TDS; IOS-2202271, to SES; and IOS-2202273, to TPE; as well as Discovery Grant RG-PIN-2020-06906, awarded to PAF, from the Natural Sciences and Engineering Research Council of Canada.

Literature Cited

Adams, D.R. 1972. Olfactory and non-olfactory epithelia in the nasal cavity of the mouse, *Peromyscus*. American Journal of Anatomy 133:37–50.

Alberts, J.R. 2007. Huddling by rat pups: Ontogeny of individual and group behavior. Developmental Psychobiology 49:22–32.

Allen, H. 1882. On a revision of the ethmoid bone in the Mammalia, with special reference to the description of this bone and of the sense of smelling in the Chiroptera. Bulletin of the Museum of Comparative Zoology 10:135–171.

Apfelbach, R., D. Russ, and B.M. Slotnick. 1991. Ontogenetic changes in odor sensitivity, olfactory receptor area and olfactory receptor density in the rat. Chemical Senses 16:209–218.

Bhatnagar, K.P. 1980. The chiropteran vomeronasal organ: Its relevance to the phylogeny of bats. Pp. 289–315, *In* D.E. Wilson and A.L. Gardner (Eds.). Proceedings of the Fifth International Bat Research Conference. Texas Tech University Press, Lubbock, TX.

Bhatnagar, K.P., and F.C. Kallen. 1974a. Morphology of the nasal cavities and associated structures in *Artibeus jamaicensis* and *Myotis lucifugus*. American Journal of Anatomy 139:167–189.

Bhatnagar, K.P., and F.C. Kallen. 1974b. Cribriform plate of ethmoid, olfactory bulb and olfactory acuity in forty species of bats. Journal of Morphology 142:71–89.

Bhatnagar, K.P., and F.C. Kallen. 1975. Quantitative observations on the nasal epithelia and olfactory innervation in bats. Suggested design mechanisms for the olfactory bulb. Acta Anatomica 91:272–282.

Bloss, J., T.E. Acree, J.M. Bloss, W.R. Hood, and T.H. Kunz. 2002. Potential use of chemical cues for colony-mate recognition in the Big Brown Bat, *Eptesicus fuscus*. Journal of Chemical Ecology 28:819–834.

Camacho, J., R. Moon, S.K. Smith, J.D. Lin, C. Randolph, J.J. Rasweiler, R.R. Behringer, and A. Abzhanov. 2020. Differential cellular proliferation underlies heterochronic generation of cranial diversity in phyllostomid bats. EvoDevo 11:1–17.

Coppola, D.M., B.A. Craven, J. Seeger, and E. Weiler. 2014. The effects of naris occlusion on mouse nasal turbinate development. Journal of Experimental Biology 217:2044–2052.

Dzal, Y.A., and E.H. Gillam. 2023. The nose knows: A review of the diversity, form, and function of the external and internal features of the bat nose. Canadian Journal of Zoology 102:103–112.

Eiting, T.P., T.D. Smith, J.B. Perot, and E.R. Dumont. 2014a. The role of the olfactory recess in olfactory airflow. Journal of Experimental Biology 217:1799–1803.

Eiting, T.P., T.D. Smith, and E.R. Dumont. 2014b. Olfactory epithelium in the olfactory recess: A case study in New World leaf-nosed bats. Anatomical Record 297:2105–2112.

Eiting, T.P., T.D. Smith, N.G. Forger, and E.R. Dumont. 2023. Neuronal scaling in the olfactory system of bats. Anatomical Record 306:2781–2790.

Gignac, P.M., N.J. Kley, J.A. Clarke, M.W. Colbert, A.C. Morhardt, D. Cerio, I.N. Cost, P.G. Cox, J.D. Daza, C.M. Early, M.S. Echols, R.M. Henkelman, A.N. Herdina, C.M. Holliday, Z. Li, K. Mahlow, S. Merchant, J. Müller, C.P. Orsbon, D.J. Paluh, M.I. Thies, H.P. Tsai, and L.M. Witmer. 2016. Diffusible iodine-based contrast-enhanced computed tomography (diceCT): An emerging tool for rapid, high-resolution, 3-D imaging of metazoan soft tissues. Journal of Anatomy 228:889–909.

Green, P.A., B. Van Valkenburgh, B. Pang, D. Bird, T. Rowe, and A. Curtis. 2012. Respiratory and olfactory turbinal size in canid and arctoid carnivorans. Journal of Anatomy 221:609–621.

Harkema, J. R., S.A. Carey, and J.G. Wagner. 2006. The nose revisited: A brief review of the comparative structure, function, and toxicologic pathology of the nasal epithelium. Toxicologic Pathology 34:252–269.

Hedrick, B.P., and E.R. Dumont. 2018. Putting the leaf-nosed bats in context: A geometric morphometric analysis of three of the largest families of bats. Journal of Mammalogy 99:1042–1054.

Hedrick, B.P., L. Yohe, A. Vander Linden, L.M. Dávalos, K. Sears, A. Sadier, S.J. Rossiter, K.T Davies, and E. Dumont. 2018. Assessing soft-tissue shrinkage estimates in museum specimens imaged with diffusible iodine-based contrast-enhanced computed tomography (diceCT). Microscopy and Microanalysis 24:284–291.

Hogan A.V., A. Watanabe, A.M. Balanoff, and G.S. Bever. 2020. Comparative growth in the olfactory system of the developing chick with considerations for evolutionary studies. Journal of Anatomy 237:225–240.

Howland, H.C., S. Merola, and J.R. Basarab. 2004. The allometry and scaling of the size of vertebrate eyes. Vision Research 44:2043–2065.

Ito, K.,V.T. Tu, T.P. Eiting, T. Nojiri, and D. Koyabu. 2021. On the embryonic development of the nasal turbinals and their homology in bats. Frontiers in Cell and Developmental Biology 9:613545.

Jones, K.E., and A. Purvis. 1997. An optimum body size for mammals? Comparative evidence from bats. Functional Ecology 11:751–756.

Kilgour, R.J., P.A. Faure, and R.M. Brigham. 2013. Evidence of social preferences in Big Brown Bats (*Eptesicus fuscus*). Canadian Journal of Zoology 91:756–760.

Loo, S.K. 1974. Comparative study of the histology of the nasal fossa in four primates. Folia Primatologica 21:290–303.

Martinez, Q., R. Lebrun, A.S. Achmadi, J.A. Esselstyn, A.R. Evans, L.R. Heaney, R. Portela Miguez, K.C. Rowe, and P.H. Fabre. 2018. Convergent evolution of an extreme dietary specialization, the olfactory system of worm-eating rodents. Scientific Reports 8:17806.

Martinez, Q., J. Clavel, J.A. Esselstyn, A.S. Achmadi, C. Grohé, N. Pirot, and P.H. Fabre. 2020. Convergent evolution of olfactory and thermoregulatory capacities in small amphibious mammals. Proceedings of the National Academy of Sciences 117:8958–8965.

Mayberry, H.W., and P.A. Faure. 2014. Morphological, olfactory, and vocal development in Big Brown Bats. Biology Open 4:22–34.

Nummela, S. 1995. Scaling of the mammalian middle ear. Hearing Research 85:18–30.

Owerkowicz, T., C. Musinsky, K.M. Middleton, and A.W. Crompton. 2015. Respiratory turbinates and the evolution of endothermy in mammals and birds. Pp. 143–165, *In* K.P. Dial, N. Shubin, and E.L. Brainerd (Eds.). Great Transformations in Vertebrate Evolution. University of Chicago Press, Chicago, IL.

Pedersen, S.C. 1993. Cephalometric correlates of echolocation in the Chiroptera. Journal of Morphology 218:85–98.

Pedersen, S.C. 1995. Cephalometric correlates of echolocation in the Chiroptera: II. Fetal development. Journal of Morphology 225:107–123.

R Core Team. 2024. The R project for statistical computing. Available online at https://www.R-project.org. Accessed 11 November 2023.

Ruf, I. 2020. Ontogenetic transformations of the ethmoidal region in Muroidea (Rodentia, Mammalia): New insights from perinatal stages. Vertebrate Zoology 70:383–415.

Santana, S.E. 2018. Comparative anatomy of bat jaw musculature via diffusible iodine-based contrast-enhanced computed tomography. Anatomical Record 301:267–278.

Santana, S.E., and K.E. Miller. 2016. Extreme postnatal scaling in bat feeding performance: A view of ecomorphology from ontogenetic and macroevolutionary perspectives. Integrative and Comparative Biology 56:459–468.

Smith, T.D., and K.P. Bhatnagar. 2004. Microsmatic primates: Reconsidering how and when size matters. Anatomical Record 279B:24–31.

Smith, T.D., and J.B. Rossie. 2008. The nasal fossa of mouse and dwarf lemurs (Primates, Cheirogaleidae). Anatomical Record 291:895–915.

Smith, T.D., K.P. Bhatnagar, J.B. Rossie, B.A. Docherty, A.M. Burrows, G.M. Cooper, M.P. Mooney, and M.I. Siegel. 2007. Scaling of the first ethmoturbinal in nocturnal strepsirrhines: Olfactory and respiratory surfaces. Anatomical Record 290:215–237.

Smith, T.D., T.P. Eiting, C.J. Bonar, and B.A. Craven. 2014. Nasal morphometry in marmosets: Loss and redistribution of olfactory surface area. Anatomical Record 297:2093–2104.

Smith, T.D., T.P. Eiting, and K.P. Bhatnagar. 2015. Anatomy of the nasal passages in mammals. Pp. 37–62, *In* R.L. Doty (Ed.). Handbook of Olfaction and Gustation. 3rd Ed. Wiley, New York, NY.

Smith, T.D., M.C. Martell, J.B. Rossie, C.J. Bonar, and V.B. Deleon. 2016. Ontogeny and microanatomy of the nasal turbinals in lemuriformes. Anatomical Record 299:1492–1510.

Smith, T.D., B.A. Craven, S.M. Engel, C.J. Bonar, and V.B. DeLeon. 2019. Nasal airflow in the Pygmy Slow Loris (*Nycticebus pygmaeus*) based on a combined histological, computed tomographic and computational fluid dynamics methodology. Journal of Experimental Biology 222(23):jeb207605.

Smith, T.D., A. Curtis, K.P. Bhatnagar, and S.E. Santana. 2021a. Fissures, folds, and scrolls: The ontogenetic basis for complexity of the nasal cavity in a fruit bat (*Rousettus leschenaultii*). Anatomical Record 304:883–900.

Smith, T.D., H.M. Corbin, S.E. King, K.P. Bhatnagar, and V.B. DeLeon. 2021b. A comparison of diceCT and histology for determination of nasal epithelial type. PeerJ 9:e12261.

Stanchak, K.E., P.A. Faure, and S.E. Santana. 2023. Ontogeny of cranial musculoskeletal anatomy and its relationship to allometric increase in bite force in an insectivorous bat (*Eptesicus fuscus*). Anatomical Record 306:2842–2852

Van Valkenburgh, B., A. Curtis, J.X. Samuels, D. Bird, B. Fulkerson, J. Meachen-Samuels, G.J. Slater. 2011. Aquatic adaptations in the nose of carnivorans: Evidence from the turbinates. Journal of Anatomy 218:298–310.

Van Valkenburgh, B., B. Pang, D. Bird, A. Curtis, K. Yee, C. Wysocki, and B.A. Craven. 2014. Respiratory and olfactory turbinals in feliform and caniform carnivorans: The influence of snout length. Anatomical Record 297:2065–2079.

Yee, K.K., B.A. Craven, C.J. Wysocki, and B. Van Valkenburgh. 2016. Comparative morphology and histology of the nasal fossa in four mammals: Gray Squirrel, Bobcat, Coyote, and White-tailed Deer. Anatomical Record 299:840–852.

Wagner, F., and I. Ruf. 2021. "Forever young"—Postnatal growth inhibition of the turbinal skeleton in brachycephalic dog breeds (*Canis lupus familiaris*). Anatomical Record 304:154–189.

Weiler, E., and A.I. Farbman. 1997. Proliferation in the rat olfactory epithelium: Age-dependent changes. Journal of Neuroscience 17:3610–3622.